



# A feasibility study of HFO refrigerants for onboard BOG liquefaction processes

Taejong Yu <sup>a</sup>, Donghoi Kim <sup>b</sup>, Truls Gundersen <sup>c</sup>, Youngsub Lim <sup>a,d,\*</sup>

<sup>a</sup> Department of Naval Architecture and Ocean Engineering, Seoul National University, 1 Gwanak-ro, Gwanak-gu, Seoul, 08826, Republic of Korea

<sup>b</sup> SINTEF Energy Research Sem Sælands Vei 11, NO-7465, Trondheim, Norway

<sup>c</sup> Department of Energy and Process Engineering, Norwegian University of Science and Technology (NTNU), Kolbjørn Hejes Vei 1B, NO-7491, Trondheim, Norway

<sup>d</sup> Research Institute of Marine Systems Engineering, Seoul National University, 1 Gwanak-ro, Gwanak-gu, Seoul, 08826, Republic of Korea

## ARTICLE INFO

Handling Editor: Wojciech Stanek

### Keywords:

LNG carrier  
Boil-off gas  
Re-liquefaction  
Optimization  
HFO refrigerant  
TNT equivalency method  
Global warming potential

## ABSTRACT

As the global demand for natural gas continues to increase, the production of liquefied natural gas (LNG) and the demand for LNG carriers are also on the rise. Following the advent of LNG propulsion engines, there has been widespread adoption of systems that use LNG or boil-off gas (BOG) as fuel, and subsequently re-liquefy remaining gas through the re-liquefaction system. In this study, we investigated the feasibility of hydrofluoro-olefins (HFO) refrigerants, the newly developed refrigerants having low flammability and low global warming potential (GWP), in BOG re-liquefaction systems for liquefied natural gas carriers. Simulations of BOG re-liquefaction process were conducted and optimized to minimize energy consumption. Then, the explosion risk and global warming potential during the lifespan of the re-liquefaction processes are also analyzed. The optimization results indicate that using HFO refrigerants in the re-liquefaction process yields comparable energy consumption to the conventional hydrocarbon refrigerants. Additionally, the use of HFO refrigerants can contribute to reducing explosion risk of liquefaction process. However, despite HFO refrigerants being considered an environmentally friendly refrigerant, it is important to note that global warming impact has not decreased as significantly as expected. This is primarily due to the fact that the GWP of the system is heavily influenced by energy consumption.

## 1. Introduction

As the demand for clean energy continues to rise, there is a growing demand for natural gas due to its relative affordability and sustainability compared to another fossil fuel [1]. To transport natural gas over long distances in a cost-effective manner, it is advantageous to convert it to a liquid form and transport it via LNG (liquefied natural gas) carriers [2]. As a result, the demand for LNG carriers is also increasing. According to world LNG report 2023 [3], the global LNG fleet grew by 10% year-on-year in 2021. When transporting LNG via vessels, LNG is stored in cargo tanks at about  $-160\text{ }^{\circ}\text{C}$  at atmospheric pressure [4]. Although there is significant insulation for an LNG cargo tank, some heat is inevitably introduced during transportation, leading to the vaporization of a portion of the LNG to form boil-off gas (BOG). Proper removal of BOG is necessary as it can increase the pressure within the cargo tank.

Currently, new systems that use liquefied natural gas (LNG) and boil-

off gas (BOG) as fuel for ship propulsion and generating power have been commercialized for LNG carriers and LNG-fueled ships [5]. The BOG can be sent to a gas combustion unit, but burning valuable natural gas is neither an economical solution nor an environment-friendly solution. Although BOG is used as fuel, surplus BOG may remain for large LNG carriers. Since the remaining BOG is essentially part of the commodity (LNG), releasing it into the atmosphere leads to economic losses and environment harm [6,7]. Consequently, a range of re-liquefaction systems have been recently explored to liquefy BOG and recirculate it back to the LNG cargo tank. This approach represents an optimal solution that can minimize both economic losses and environmental harm.

To liquefy BOG, external refrigerants are commonly used. There are two types of conventional and traditional refrigerant for BOG liquefaction. One is nitrogen (N<sub>2</sub>) used in the reverse Brayton cycle and the other is mixed hydrocarbons used in the mixed refrigerant (MR) cycle. These processes have been studied by many researchers [8–15]. One

\* Corresponding author. Department of Naval Architecture and Ocean Engineering, Seoul National University, 1 Gwanak-ro, Gwanak-gu, Seoul, 08826, Republic of Korea.

E-mail address: [s98thesb@snu.ac.kr](mailto:s98thesb@snu.ac.kr) (Y. Lim).

<https://doi.org/10.1016/j.energy.2023.128980>

Received 4 November 2022; Received in revised form 29 August 2023; Accepted 31 August 2023

Available online 1 September 2023

0360-5442/© 2023 The Authors. Published by Elsevier Ltd. This is an open access article under the CC BY-NC license (<http://creativecommons.org/licenses/by-nc/4.0/>).

advantage of using the N2 reverse Brayton cycle is that N2 is safe compared to other refrigerants, since it is not an explosive material, but N2 reverse Brayton cycles usually have relatively low efficiency. On the other hand, hydrocarbons can reduce the energy consumption of the liquefaction process, by using various components having different boiling points and specific heat capacities [16]. Yin et al. [17] compared mixed refrigerants and an N2 expander liquefaction cycle and reported that the N2 expander cycle consumes more than twice the compression energy of the mixed refrigerant cycle. However, hydrocarbons are highly flammable materials that are classified in the A3 group in the refrigerant safety classification of the American Society of Heating, Refrigerating and Air-conditioning Engineers (ASHRAE), as shown in Table 1 [18,19]. In the case of hydrocarbons, the damage in the event of an explosion could be quite great.

To maintain the energy efficiency of hydrocarbons and ensure the safety of N2, there have been studies that use non-flammable refrigerants such as chlorofluorocarbons (CFCs), hydrofluorocarbons (HFCs) and hydrochlorofluorocarbons (HCFCs). The efficiency of cycles using these refrigerants is comparable with the hydrocarbon (HC) based mixed refrigerant cycles and there is no explosion potential. However, most of the nonflammable refrigerants are man-made chemicals, and it has been reported that they damage global environmental conditions. CFCs and HCFCs damage the ozone layer of the earth, which can be evaluated by the Ozone Depletion Potential (ODP) that is defined as the relative amount of degradation the material can cause to the ozone layer compared to 1 kg of CFC-11. HFCs and HCFCs that accelerate the global warming effect significantly, can be evaluated by the Global Warming Potential (GWP) that is a measure of how much a given mass of a gas contributes to global warming compared to 1 kg of CO2 as shown in Table 2. As a result, the use of CFC, HFC, and HCFC, has been restricted or is going to be restricted by regulations [20].

Taking into account these considerations, Hydrofluoro-olefin (HFO) is a newly developed refrigerant to respond to environmental regulations in refrigerant use. The HFOs possess double bonds in their molecular structure, which render them highly susceptible to decomposition in the air. Consequently, they have minimal environmental impact, leading to low GWP and ODP [21]. Moreover, HFOs have lower flammability than hydrocarbons; they are classified in the A2L group by ASHRAE, which means that the material has a heat of combustion of less than 19,000 kJ/kg and a burning velocity of less than 10 cm/s as shown in Table 1. As indicated in Table 2, HFOs exhibit reduced flammability in comparison to hydrocarbons, and lower GWP values in comparison to non-flammable refrigerants. In summary, HFO refrigerants have the potential to replace conventional refrigerants for BOG liquefaction due to their potential to reduce energy consumption compared to N2, lower explosion risk compared to hydrocarbons, and reduced environmental impact compared to non-flammable refrigerants.

There exist studies investigating the use of HFO refrigerants in the liquefaction process. Specifically, Qyyum and Lee [22], and Ali et al. [23] utilized HFO-MR in LNG production, while Naquash et al. [24] and Lee et al. [25] incorporated HFO refrigerants into conventional

hydrocarbon MR during the pre-cooling stage of hydrogen liquefaction. These studies indicate that the addition of HFO refrigerants to hydrocarbon mixture can potentially reduce energy consumption in liquefaction processes. However, it should be noted that these studies solely added HFO refrigerants to conventional hydrocarbon mixture and evaluated only the energy consumption of the process.

In this study, we aim to evaluate the feasibility of HFO refrigerants as a replacement for hydrocarbons in the BOG re-liquefaction process. Our objective is to compare BOG re-liquefaction systems utilizing HFO with conventional hydrocarbon-based processes from the perspectives of energy consumption, explosion risk, and environmental impact. BOG re-liquefaction processes are modeled and optimized to minimize energy consumption. After the optimization, the overpressure and GWP of optimized model are estimated to investigate the impacts on the risk of explosion and global warming. For a more accurate analysis, not only the GWP of the refrigerant, but also the amount of GWP generated by considering refrigerant leakage, the amount of CO2 generated by energy consumption, and the GWP generated by disposal during the lifespan were estimated.

## 2. Background

The MR liquefaction process has been widely used for commercial natural gas liquefaction. It has smaller temperature differences between the hot and cold composite curves in the main heat exchanger than other natural gas liquefaction processes such as the N2 expander or cascade cycle, resulting in reduced heat loss from the heat exchanger and lower energy consumption [26]. Typically, mixed refrigerants are composed of nitrogen and hydrocarbons ranging from C1 to C4 [27]. A simplified process diagram of a single mixed refrigerant (SMR) natural gas liquefaction process without a phase separator is shown in Fig. 1 [28]. It consists of a multi-stage compressor with inter-coolers and one multi-stream heat exchanger. As the name indicates, the SMR process has a single cycle, so it is relatively simple compared to other MR processes, resulting in low equipment cost and fixed cost [27,29]. On the other hand, the dual mixed refrigerant (DMR) natural gas liquefaction process, shown in Fig. 2 [15], requires a larger number of units and a more complex configuration, but the two independent cycles can provide more efficient heat exchange between natural gas and refrigerants, resulting in smaller energy consumption than the SMR process.

Natural gas liquefaction is very energy intensive, and energy consumption varies greatly depending on operating conditions [30]. Hence, it is important to optimize the operating conditions of the process to avoid excessive energy consumption. Natural gas liquefaction is a complex process that has multiple variables and high non-linearity, hence the optimization algorithm should be carefully selected to find an optimal solution [31]. Particle swarm optimization (PSO) [32,33] is one of the most widely used algorithms for global optimization. Similar to the genetic algorithm (GA), the PSO algorithm is an optimization tool based on population. The system is initialized with a population of random solutions and it can search for optimal by updating generations. It is a non-calculus-based method and can solve discontinuous, multi-modal and non-convex problems [34]. The objective function for the optimization in this study is specific energy consumption (SEC) as shown in Eq. (1), which is a commonly used key performance indicator to compare the efficiency of liquefaction processes [35].

$$\text{SEC} [\text{kWh} / \text{kg}] = \frac{\dot{W}_{\text{comp}}}{\dot{m}_{\text{LNG}}} \quad (1)$$

where  $\dot{W}_{\text{comp}}$  is refrigerant compression power (kW) and  $\dot{m}_{\text{LNG}}$  is LNG production rate (kg/hr).

Explosions are a major hazard of process systems, often causing significant fatalities and damage to property. A common definition of an explosion is that a sudden expansion of matter to a much larger volume than it formerly occupied causes rapid change in pressure of the

**Table 1**  
ASHRAE refrigerant safety classification.

Group	Flammability	Lower flammable limit (@23 °C, 101.3 kPa)	Heat of combustion (@23 °C, 101.3 kPa)	Burning velocity (@23 °C, 101.3 kPa)
A1	No flame propagation	–	–	–
A2L	Lower flammable	≥3.5% vol.	<19,000 kJ/kg	≤10 cm/s
A2	Flammable	≥3.5% vol.	<19,000 kJ/kg	–
A3	Higher flammable	<3.5% vol.	≥19,000 kJ/kg	–

**Table 2**  
Properties of refrigerants.

Refrigerant	Type	Boiling point [°C]	Heat of combustion [kJ/kg] (@23 °C, 101.3 kPa)	Safety class	GWP	ODP
Methane	Hydrocarbon	-161.6	55,510	A3	25	0
Ethane	Hydrocarbon	-89	51,900	A3	6	0
Propane	Hydrocarbon	-42	50,330	A3	3	0
Butane	Hydrocarbon	-1	49,500	A3	4	0
HFO1234yf	HFO	-30	10,700	A2L	1	0
HFO1234ze	HFO	-18.95	10,700	A2L	0	0
HFO1233zd	HFO	18.3	Non-flammable	A1	1	0
R-11	CFC	23.77	Non-flammable	A1	4660	1
R-12	CFC	-29.8	Non-flammable	A1	10,200	1
R-22	HCFC	-40.7	Non-flammable	A1	1760	0.05
R-123	HCFC	27.6	Non-flammable	A1	79	0.02
R134a	HFCs	-26.3	Non-flammable	A1	1300	0
R404a	HFCs	-46.6	Non-flammable	A1	3922	0

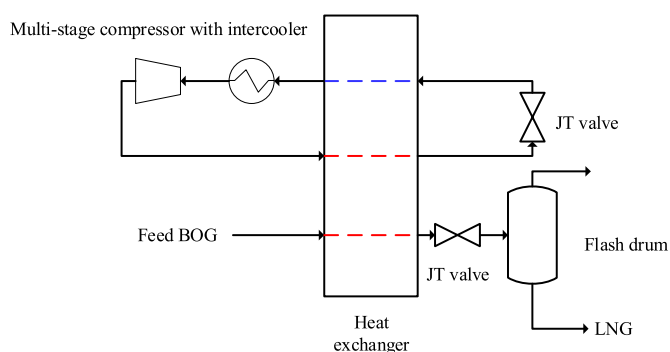


**Fig. 1.** Single mixed refrigerant (SMR) cycle.

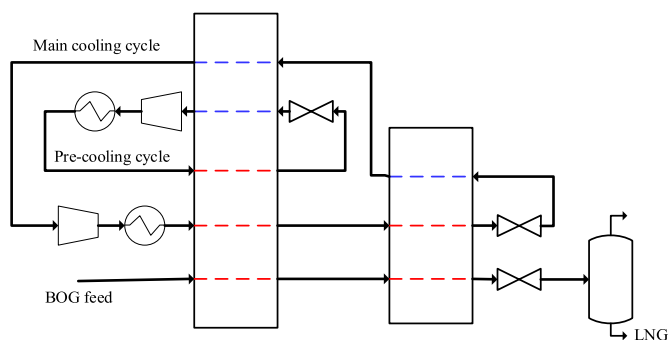


**Fig. 2.** Dual mixed refrigerant (DMR) cycle.

surroundings [36]. The blast effects of an explosion are in the form of a shock wave composed of a high-pressure shock front, which expands outward from the center of the detonation with maximum overpressure decaying with distance. Therefore, overpressure is one of the most important factors concerning the magnitude of an explosion, and it is responsible for damage to humans, structures and environmental elements. One simple method for assessing overpressure caused by the explosion is the trinitrotoluene (TNT) equivalency method [37]. The model calculates the TNT equivalent mass ( $W_{TNT}$ ), which is the mass of TNT with the same effect as the amount involved in the explosion. Overpressure is obtained as a function of  $W_{TNT}$  and distance from the explosion center. Fig. 3 briefly shows the procedure of the TNT equivalent method to assess overpressure. With this procedure, we evaluate the explosion risk of simulated processes.

### 3. Methodology

To investigate HFO refrigerants in the BOG re-liquefaction process,

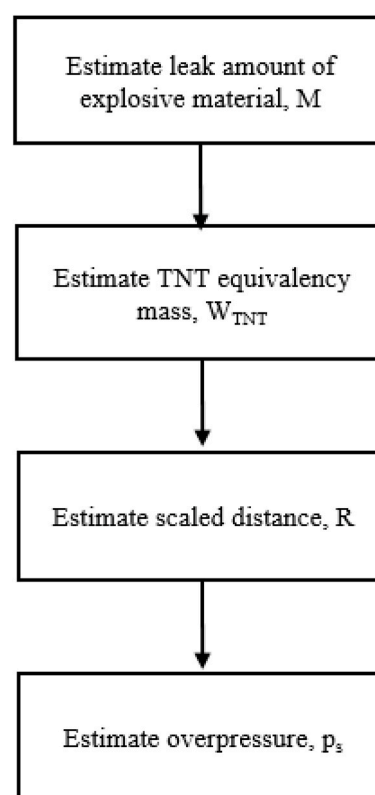


**Fig. 3.** Procedure for the TNT equivalency method.

we simulated the BOG re-liquefaction process using Aspen HYSYS V10, the chemical process simulator used widely in industrial and academic fields. We modeled a BOG re-liquefaction system including BOG generation, fuel gas supply for the main engine and generator, and BOG re-liquefaction process. Then, we optimized the energy consumption of the process with operating conditions such as composition of mixed refrigerants, temperature, and compressor pressure. After optimization, we estimated the overpressure and the total GWP of process. The overpressure results from explosion accidents due to refrigerant leakage. In this procedure, the TNT equivalency model is used. When estimating the total GWP during the lifespan of the process. We considered refrigerant leakage, CO<sub>2</sub> emissions while supplying the energy required for the process and disposal of refrigerant. The details of each procedure are as follows.

#### 3.1. Modeling

To decide the BOG generation rate, this study selected a target vessel

of an LNG carrier having the capacity of 170,000 m<sup>3</sup>, which was the most common size of new LNG carriers built in 2019 [2]. It is assumed that LNG is in saturated liquid condition at an operating pressure of 1.06 bar and a temperature of −160.8 °C. It is further assumed that LNG is filled up to 95% of the tank volume to give a margin for volume and pressure increase due to BOG generation [6]. Peng-Robison equation is used as an equation of state to calculate thermodynamic properties and simulate the processes.

The composition of LNG is assumed to be as shown in Table 3.

The BOR (Boil-off ratio) is assumed to be 0.1 wt% of the amount of storage per day [38], and then the BOG generation rate is calculated using Eq. (2). The BOG inlet temperature is assumed to be −125 °C [39]. Table 4 shows the properties of BOG resulting from the simulation.

$$\dot{m}_{\text{BOG}} = \frac{\text{BOR} \cdot \rho \cdot V}{24} \quad (2)$$

where  $\dot{m}_{\text{BOG}}$  is BOG generation rate (kg/hr),  $\rho$  is the density of LNG (kg/m<sup>3</sup>) and  $V$  is the volume (m<sup>3</sup>) of stored LNG in the tank.

Fig. 4 shows the overall process flow diagram of a BOG re-liquefaction system based on the SMR cycle. Generated BOG flows into compressors (K-1, K-2) and the pressure is increased to 11.5 bar. After cooling (E-1), stream B3 is sent to the power generation engine, and the remaining BOG (B2) is compressed to 17.1 bar. A part of the stream is sent to the propulsion engine (B4). Then the remaining BOG (B5) is liquefied through the re-liquefaction process. The compressor efficiency is assumed at 75% and the cooling temperature of the inter-cooler is set to 40 °C.

To determine the BOG consumption rate for the main propulsion engine and auxiliary power generation engine, it is assumed that two types of engines are installed: a low pressure two-stroke dual fuel engine for propulsion and a dual fuel diesel engine (DFDE) for generating electricity for use in the ship. Two 11,925 kW WinGD X-62DF engines [40] are used as propulsion engines, and an 8000 kW Wartsila 16V34DF engine [41] is used for power generation. To estimate the required amount of gas for each engine, Eq. (3) is used. The corresponding assumed values of each engine are shown in Table 5.

$$\dot{m}_{\text{fuel}} = \frac{P_e \cdot \text{SFOC} \cdot l}{\text{LHV}} \quad (3)$$

where  $\dot{m}_{\text{fuel}}$  is the fuel consumption in kg/hr,  $P_e$  is the engine power in kW, SFOC is the specific fuel oil consumption in kJ/kWh, LHV is the lower heating value of BOG in kJ/kg based on the BOG composition, and  $l$  is the engine load in %.

The BOG stream (B5) is liquefied by heat exchange with the MR cycle. The MR (R1) is compressed with inter-cooling and sent to the heat exchanger for cooling. The cooled MR (R6) expands in the Joule-Thomson valve and reaches cryogenic temperature. The MR then flows into the heat exchanger to cool down the refrigerant itself and the BOG. The BOG is cooled through the heat exchanger and then expanded to 2 bar reaching −162.2 °C. About 8% of the liquefied BOG is vaporized through the valve, separated in the flash drum and used for power generation in the liquefaction process.

The SMR BOG re-liquefaction system using HFO MR could have one potential problem related to the freezing point of HFO 1233zd, which is −106 °C at ambient pressure. Although the freezing point can be lower as part of a mixed refrigerant, freezing may occur in the SMR

**Table 3**  
Composition of LNG stored in tank.

Parameters	Unit	Value
Nitrogen	mol%	0.37
Methane	mol%	95.89
Ethane	mol%	2.96
Propane	mol%	0.72
Normal butane	mol%	0.06

**Table 4**  
Properties of the BOG.

Parameters	Unit	Value
Nitrogen	mol%	8.76
Methane	mol%	91.23
ethane	mol%	0.01
BOG pressure	bara	1.06
BOG temperature	°C	−125
BOG flowrate	kg/hr	2938

liquefaction process when the MR is cooled down to severe cryogenic temperatures around −160 °C. In order to prevent this problem, the dual mixed refrigerant (DMR) cycle is also considered, as shown in Fig. 5. The DMR process consists of two refrigerant cycles. Warm refrigerant is used for pre-cooling of BOG and cold refrigerant is used for condensation of BOG. Similar to the SMR BOG re-liquefaction system, the refrigerant is compressed with inter-cooling. The compressed refrigerant streams, WR5 and CR5, are sent to the heat exchanger HEX-1 and cooled. The cooled refrigerants, WR6 and CR7, expand through Joule-Thomson valves, VLV-1 and VLV-2 and flow into the heat exchangers to supply cooling duty. HFO1233zd is not included in the cold MR cycle to avoid potential freezing problems.

### 3.2. Optimization

As presented in the background part, the specific energy consumption (Eq. (1)) is minimized by linking Aspen HYSYS V10 [42] with MATLAB R2019b [43]. Aspen HYSYS is a process simulation software widely used in the field of chemical engineering and MATLAB is a programming language and numerical computing environment commonly used in engineering and science. In this study, MATLAB generates the values of the process variables through the PSO algorithm to optimize the energy consumption of the process. Subsequently, these values are transmitted to Aspen HYSYS. In Aspen HYSYS, the BOG re-liquefaction process is simulated, and thermodynamic properties of its stream and results of each equipment operation are calculated. Then, SEC is estimated by following Eq. (1). The obtained result is then conveyed back to MATLAB for searching the next optimal points. Below Fig. 6 shows how Aspen HYSYS and MATLAB work.

Table 6 shows simulation cases and process variables for each case. With the SMR process, 2 cases of simulation and optimization were performed. Case 1 is a reference case using conventional refrigerants with hydrocarbons and nitrogen. Case 2 uses the suggested HFO refrigerants for BOG re-liquefaction. However, since HFO refrigerants have boiling points from −30 °C to 18.3 °C, methane and ethane are kept as refrigerants together with HFOs in Case 2. Case 3 uses the DMR cycle and HFO1233zd is removed from the cold MR cycle to avoid potential freeze-out problems.

The compression ratio is constrained to be below 4 and the vapor fraction at the compressor inlet should be 1 to avoid liquid being sent to the compressor. The minimum approach temperature of heat exchangers is specified to 3 °C.

### 3.3. Risk assessment

After optimization, overpressure is estimated using the TNT equivalent method. Overpressure is estimated for all refrigerant streams based on their pressure, temperature, composition and phase. First, it is assumed that an explosive substance leaks from an equipment or pipe and forms a vapor cloud. The leakage rate is a function of the hole size and the working conditions. Liquid and vapor leakage rates are obtained from Eq. (4) [44] and Eq. (5) [45].

$$Q_L = C_{\text{liquid}} A \sqrt{2\rho_L(P_I - P_a)} \quad (4)$$

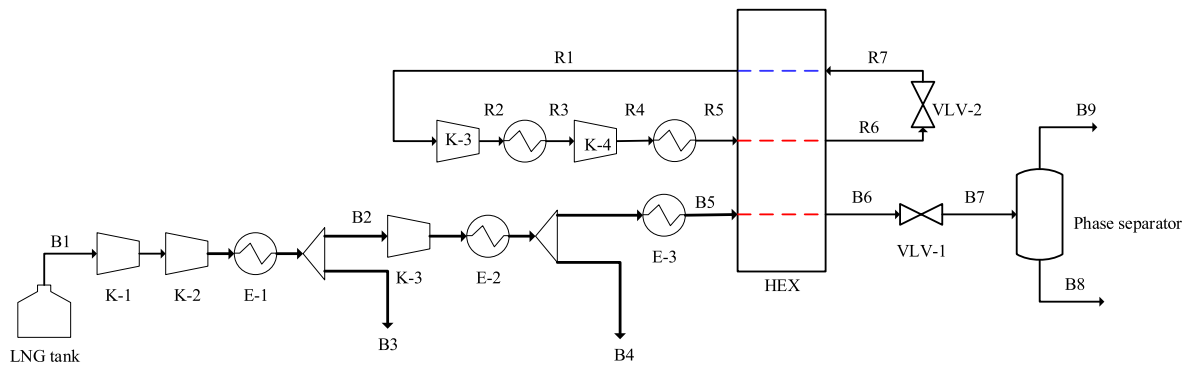


Fig. 4. Fuel gas supply system and BOG re-liquefaction process based on an SMR cycle.

Table 5  
Engine specification.

Parameter	Unit	Main engine	Aux. engine
Power	kW	11,925 x 2	8000
SFOC	kJ/kWh	7132	7679
Load	%	40	50
LHV	kJ/kg	42,900	
Fuel consumption	kg/h	1586	716

where  $Q_L$  and  $Q_V$  are leakage rates of liquid phase and vapor phase in

$$Q_V = \begin{cases} C_{\text{gas}} A P_I \sqrt{\frac{\gamma M_w}{R_g T_s} \left(\frac{2}{\gamma+1}\right)^{\frac{\gamma+1}{\gamma}}} \text{ for sonic flow } \left(\frac{2}{\gamma+1}\right)^{\frac{\gamma}{\gamma+1}} \geq \left(\frac{P_a}{P_I}\right) \\ C_{\text{gas}} A P_I \sqrt{\frac{\gamma M_w}{R_g T_s} \left(\frac{\gamma}{\gamma+1}\right) \left[\left(\frac{P_a}{P_I}\right)^{\frac{2}{\gamma}} - \left(\frac{P_a}{P_I}\right)^{\frac{\gamma+1}{\gamma}}\right]} \text{ for subsonic flow } \left(\frac{2}{\gamma+1}\right)^{\frac{\gamma}{\gamma+1}} < \left(\frac{P_a}{P_I}\right) \end{cases} \quad (5)$$

kg/s,  $A$  is the area of the leak hole in  $\text{m}^2$ . A diameter of 3 mm is assumed [46].  $C$  is the discharge coefficient; 0.85 for gas and 0.61 for liquid.  $\rho_L$  is the liquid density in  $\text{kg}/\text{m}^3$ ,  $P_I$  is the absolute pressure inside the pipe in Pa,  $P_a$  is the atmospheric pressure in Pa,  $M_w$  is the molecular weight, and  $\gamma$  is the ratio of specific heat capacities.

Total leakage of flammable material can be calculated by Eq. (6).

$$M = [(xQ_{V\text{leak}} + (1-x)Q_{L\text{leak}})]t \quad (6)$$

where  $x$  is the vapor fraction,  $M$  refers to the amount of leakage in kg,

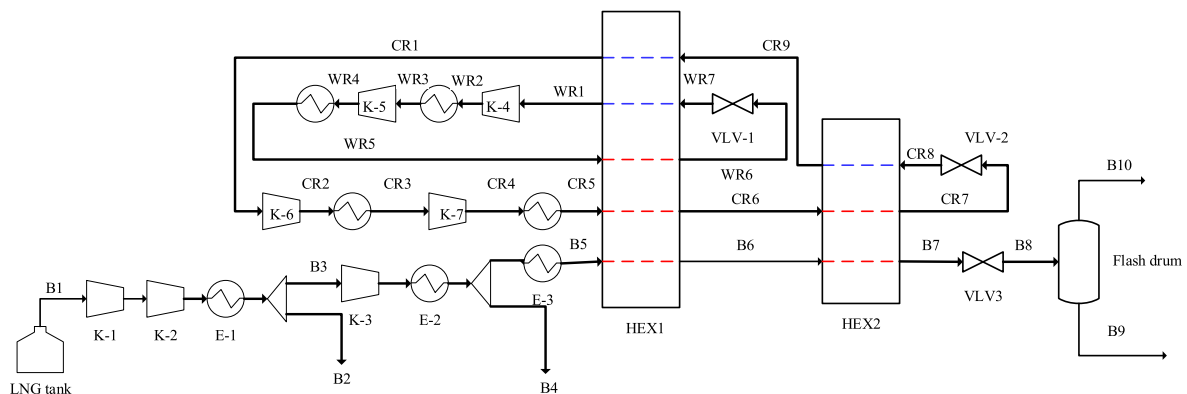


Fig. 5. BOG re-liquefaction process based on the DMR cycle.

and  $t$  is the time in seconds. The time  $t$  is assumed to be 90 s, equivalent to the total working time of the emergency shutdown system [44].

From the calculated amount of leakage, the TNT equivalent mass ( $W$ ) and scaled distance ( $Z$ ) can be calculated by Eqs. (7)–(9).

$$W = \frac{\eta M E_c}{E_{TNT}} \quad (7)$$

where  $W$  is the equivalent mass of TNT in kg and  $\eta$  is the empirical explosion efficiency. The empirical explosion efficiency ( $\eta$ ) varies between 0.01 and 0.1. From a conservative perspective, it is assumed to be 0.1.  $E_c$  is the heat of combustion of flammable material in  $\text{kJ}/\text{kg}$  and  $E_{TNT}$  is the heat of combustion of TNT, 4437  $\text{kJ}/\text{kg}$ .

From the equivalent mass of TNT, the scaled distance and over-pressure caused by the explosion can be estimated by Eq. (8) and Eq. (9) [47].

$$Z = \frac{R}{W^{1/3}} \quad (8)$$

where  $Z$  is the scaled distance in  $\text{m}/\text{kg}^{1/3}$  and  $R$  is the distance from the ignition point in meters.

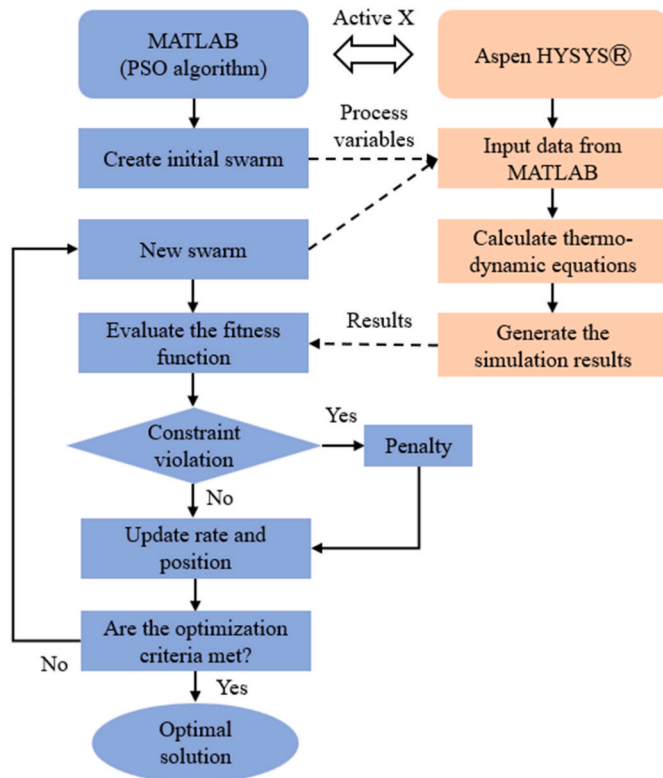


Fig. 6. Procedure for optimization with Aspen HYSYS and MATLAB.

Table 6  
Process variables depending on simulation case.

Variable	Case 1	Case 2	Case 3	
Heat exchanger	main HEX	main HEX	pre-cooling	main HEX
MR component mass flow	N2 C1 C2 C3 nC4	N2 C1 C2 HFO1234yf HFO1234ze HFO1233zd	N2 C1 C2 HFO1234yf HFO1234ze HFO1233zd	N2 C1 C2 HFO1234yf HFO1234ze
Compressor ratio	K-4, K-5		K-4, K-5, K-6, K-7	
Temperature after heat exchanger	B6		CR1, CR6, CR7, WR6, B6	
Pressure after JT expansion	R7		WR7, CR8	

$$\log_{10} P_o = \sum_{i=0}^n c_i (a + b \cdot \log_{10} Z)^i \quad (9)$$

where  $P_o$  is the overpressure in Pa.  $a$ ,  $b$  and  $i$  are the regression coefficients for estimating overpressure [47].

### 3.4. Environmental assessment

In this study, total GWP during the lifespan of an LNG carrier is estimated in three parts: (1) GWP caused by the leakage of refrigerants during operation ( $GWP_{leak}$ ), (2) GWP caused by CO2 emission for power generation ( $GWP_{CO2}$ ), and (3) GWP caused by the disposal of refrigerants ( $GWP_{disposal}$ ) after the lifespan of the ship. The lifespan of an LNG carrier is assumed to be 20 years.

The  $GWP_{leak}$  is the GWP from the leakage of refrigerants in normal operation. The amount of refrigerant leakage per year is assumed to be proportional to the refrigerant flow rate, and this quantity is estimated using Eq. (10).

$$GWP_{leak} = GWP_{MR} \cdot \dot{m}_{MR} \cdot k \quad (10)$$

where  $GWP_{leak}$  is the GWP generated by leakage of refrigerant per year,  $\dot{m}_{MR}$  is the flowrate of mixed refrigerant in the refrigeration cycle and  $k$  is the fraction of refrigerant leakage per year. The annual refrigerant leakage ( $k$ ) is assumed to be 0.05, 0.1, or 0.15. The GWP for a mixed refrigerant can be calculated by Eq. (11).

$$GWP_{MR} = \sum x_i \cdot GWP_i \quad (11)$$

where,  $GWP_{MR}$  is global warming potential of 1 kg of mixed refrigerant,  $x_i$  refers to the mass fraction of material  $i$  and  $GWP_i$  is the GWP of material  $i$ .

The  $GWP_{CO2}$  represents the GWP resulting from the emission of CO2 during the power generation process to supply the re-liquefaction system annually. This value can be determined using Eq. (12) as described in Ref. [48].

$$GWP_{CO2} = P_e \cdot EF \quad (12)$$

where  $P_e$  is the power consumed in the re-liquefaction process, and  $EF$  is the carbon emission factor of the fuel. It refers to the amount of CO2 generated to produce a unit of energy depending on the type of fuel. Assuming that LNG fuel with 46.5 GJ/t is used, the factor  $EF$  will be 61.0 [49]. Availability of the re-liquefaction process is assumed to be 50% per year.

The  $GWP_{disposal}$  refers to the GWP resulting from the disposal of refrigerants after the lifespan of the LNG carrier. The GWP value due to the disposal of the refrigerants can be estimated using Eq. (13).

$$GWP_{disposal} = GWP \cdot m_{MR} \cdot z \quad (13)$$

where  $GWP_{disposal}$  is the GWP due to the disposal of refrigerants and  $m_{MR}$  is the amount of refrigerant in the re-liquefaction process in kg.  $z$  is the percent of refrigerant disposed and is assumed to be 30% for medium and large commercial refrigeration systems [50]. To estimate the amount of refrigerant in the systems ( $m_{MR}$ ), Eq. (14) is used.

$$m_{MR} = V_{HEX} \cdot \rho_{MR} \cdot f \quad (14)$$

$V_{HEX}$  is the volume of the heat exchanger in  $m^3$  and  $\rho_{MR}$  is the density of the refrigerant mixture in kg per  $m^3$ .  $f$  is the factor to estimate total amount of refrigerant from inventory of the heat exchanger and is assumed to be 2.38 [51].

We estimate the annual GWP, which is the GWP that is generated in one year, can be obtained by Eq. (15) before GWP over life span was estimated. It consists of GWP from leakage and CO2 emission.

$$GWP_{annual} = GWP_{leak} + GWP_{CO2} \quad (15)$$

where  $GWP_{annual}$  is the GWP per year.

We then calculate the total GWP over the lifespan of the LNG carrier by multiplying  $GWP_{annual}$  by the number of years of the lifespan and adding  $GWP_{disposal}$ , as shown in Eq (16).

$$GWP_{total} = GWP_{annual} \cdot y + GWP_{disposal} \quad (16)$$

where  $y$  is the lifespan of the LNG carrier, which is assumed to be 20 years.

## 4. Results and discussion

### 4.1. Energy optimization

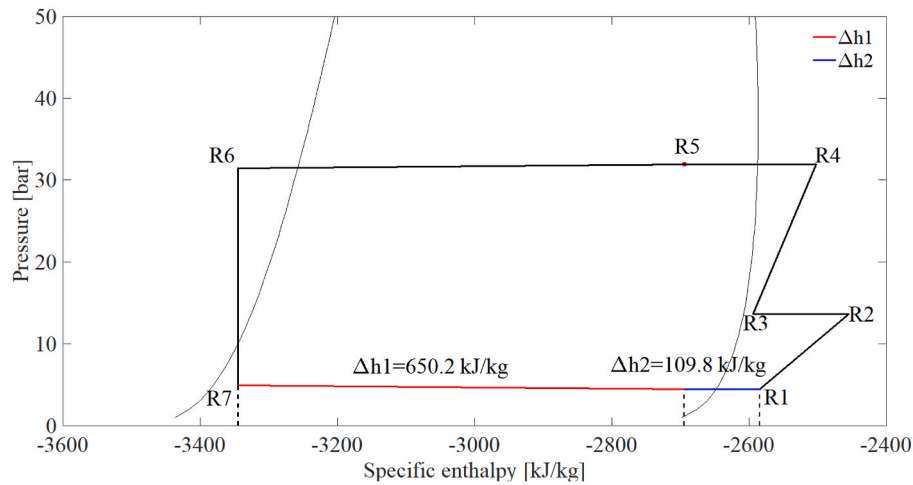
This section presents the optimization results of the re-liquefaction processes with SEC as an objective function. Subsequently, estimates of overpressure due to explosion accidents and the total GWP are presented based on the optimized solutions. In Case 1, the reference case uses HC refrigerants and the SMR process. In Case 2, a mixture of HC and

**Table 7**  
Optimized process variables.

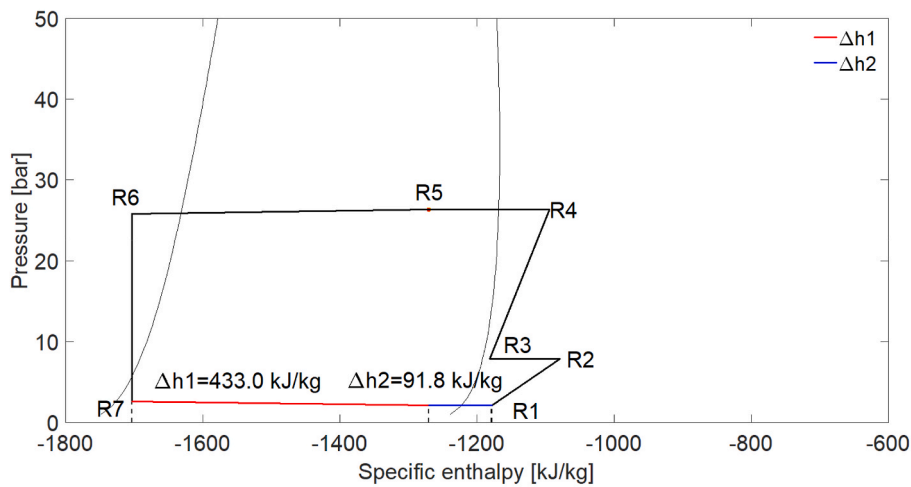
Case	Case 1		Case 2		Case 3			
Process	SMR		SMR		DMR			
Compressor ratio	K-4	3.07	K-4	3.69	K-4	2	K-6	3.99
	K-5	2.34	K-5	3.34	K-5	2.22	K-7	2.34
Temperature after heat exchanger [°C]	-154.4		-154.5		CR1	-10	WR6	-75.3
					CR6	-100	B6	-90.3
					CR7	-154.4		
Pressure after JT expansion [bar]	4.95		2.64		WR7	3.19	CR8	5

**Table 8**  
Specific energy consumption (SEC) and GWP depending on refrigerant composition.

Case	Case 1		Case 2		Case 3			
Cycle	main		main		pre-cooling		main	
MR composition	N2	11.58	N2	7.51	N2	0	N2	14.4
	C1	41.09	C1	41.13	C1	9.9	C1	52.22
	C2	22.34	C2	26.79	C2	16.09	C2	22.56
	C3	0	HFO-1234yf	2.62	HFO-1234yf	44.45	HFO-1234yf	10.04
	nC4	24.99	HFO-1234ze	0.2	HFO-1234ze	0.04	HFO-1234ze	0.78
			HFO1233zd	21.75	HFO1233zd	29.52		
MR mass flowrate [kg/kr]	4744		5675		5406		2983	
SEC [kWh/kg]	0.513		0.519		0.478			
GWP <sub>MR</sub>	8.47		5.01		4.07			



(a)



(b)

**Fig. 7.** P-h diagram of single mixed refrigerants in (a) Case 1 and (b) Case 2.

HFO refrigerants is used along with the SMR process. Case 3 replaces the SMR process with a DMR process to improve efficiency and prevent freeze-out problems of refrigerants. The SMR process operates at cryogenic temperatures, which can cause freeze-out problems in HFO refrigerants with high freezing points. In contrast, this issue can be avoided in the DMR process by limiting the use of HFO refrigerants with high freezing points to the pre-cooling cycle.

Table 7 presents the optimized process variables, while Table 8 provides information on the composition, flowrate, SEC, and GWP of the refrigerant mixture based on the results in Table 7.

The results of the study indicate that there is no significant difference in specific energy consumption (SEC) between Case 1 and Case 2. The study found that HFO refrigerants can be used as an effective replacement for hydrocarbon refrigerants in the SMR process while maintaining comparable energy efficiency. Fig. 7 provides pressure-enthalpy diagrams of single mixed refrigerants and illustrates the change in specific enthalpy required to cool down the refrigerant itself ( $\Delta h_1$ ), as well as the cold thermal energy used to liquefy the boil-off gas (BOG) ( $\Delta h_2$ ). In Case 2, the useable specific heat required to cool down the BOG is less than in Case 1, resulting in a larger mixed refrigerant (MR) flow rate for Case 2. Despite the lower refrigerant compression pressure required in Case 2, the SECs of both Case 1 and Case 2 are similar due to the larger MR flow rate in Case 2.

As expected, the more efficient DMR process has a moderately lower SEC than the two cases with SMR. Fig. 8 shows composite curves during heat exchange in Case 1 and Case 3. The DMR process cools the high-temperature BOG through pre-cooling before liquefaction in the main heat exchanger. The refrigerant used for pre-cooling is composed of a mixture with a relatively high boiling point, and a high heat exchange efficiency can be achieved by narrowing the vertical distance between the composite curves during heat exchange at higher temperatures.

To quantitatively check the reason for differences in energy consumption, analysis of logarithmic mean temperature difference (LMTD) and entropy generation in heat exchangers was performed as shown in Table 9. Several objective specifications such as LMTD and mean temperature approach (MTA) of multi stream heat exchangers can be estimated by simple weighted method [52]. In this method, the heating curves are broken into intervals and energy balance is performed on each interval as following Eq. (17).

$$m_i C_{pi} \bullet (T_{h,i} - T_{c,i}) = \sum_{j=1}^n A_{i,j} U_{i,j} (T_{m,j} - T_{m,i}) \tag{17}$$

where  $m_i$  is the flowrate of stream in the heat exchanger,  $C_{pi}$  is isobaric specific heat capacity,  $U_{i,j}$  is the overall heat transfer coefficient and  $A_{i,j}$  is the heat transfer area.

The results show that lower LMTD tends to have smaller SEC. However, the main heat exchanger in Case 3 has the largest LMTD because it focuses on the section where the phase change of BOG occurs. Thus, LMTD cannot clearly show the difference in energy consumption

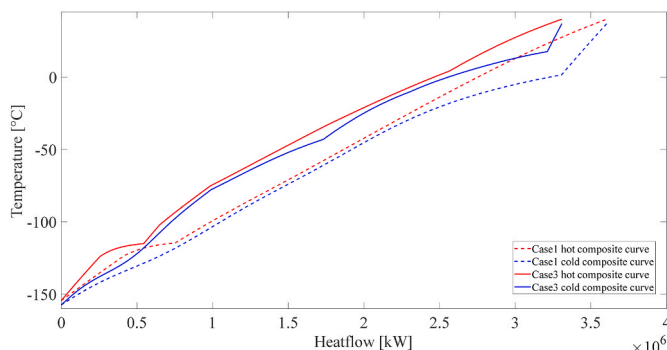


Fig. 8. Composite curves during heat exchange in Case 1 and Case 3.

Table 9

Log mean temperature difference and entropy generation in heat exchangers.

Parameter	Unit	Case 1	Case 2	Case 3 <sub>warm</sub>	Case 3 <sub>cold</sub>
LMTD	•°C	5.08	6.02	4.67	6.74
Entropy generation	W/K	206.4	215.8	107.4	82.7

in each case. On the other hand, entropy generation can show the reason for differences in energy consumption. Case 3 has the lowest entropy generation in heat exchange and therefore consumes less energy than other cases.

The difference in  $GWP_{MR}$  depends on the composition of HFO refrigerants. In Case 2 and 3, where HC was replaced by HFO refrigerants, the  $GWP_{MR}$  is smaller than that in Case 1 using the hydrocarbon mixture. The  $GWP_{MR}$  of Cases 2 and 3 decreased by 41 and 52% compared to Case 1, respectively. In Case 3, although the fractions of HCs in the cold MR are high, the required cold MR flow rate is small and the warm MR has high HFO composition with a large flow rate, resulting in the lowest  $GWP_{MR}$ .

#### 4.2. Overpressure induced by explosion accident

For fast evaluation of risk, we tried to show the relative explosion risk by using the overpressure calculated from the TNT equivalent method, instead of applying detailed risk assessment. Table 10 shows the maximum overpressure estimated among refrigerant streams. In all cases, maximum overpressure is calculated for the refrigerant streams after expansion (R7, WR7, and CR8 in Figs. 4 and 5), which have the largest liquid fraction in the cycles. Due to high liquid density, the amount of flammable material leaking from the same size of the leakage hole is larger than for vapor, and it results in the maximum overpressure. Although using HFO does not show significant improvement in energy consumption of the liquefaction processes, it greatly reduces explosive risks. The overpressure of Case 2 decreases by 33.3–49.5% compared to Case 1, depending on the distance from the ignition point. In Case 3, overpressure in the pre-cooling cycle, Case 3<sub>warm</sub>, is lower than that of Case 1. However, the main cooling cycle, Case 3<sub>cold</sub>, has similar overpressure as Case 1 due to large fractions of methane and ethane.

#### 4.3. Total global warming potentials

Table 11 shows the annual GWP with contributions from leakage and combustion without GWP from disposal of the refrigerant. As indicated,

Table 10

Maximum overpressure as function of distance.

Case	Unit	3 m	5 m	10 m	15 m	20 m
Case 1	bar	11.08	3.97	0.99	0.44	0.24
Case 2	bar	6.58	2.04	0.5	0.25	0.16
Case 3 <sub>warm</sub>	bar	3.29	1.06	0.3	0.16	0.11
Case 3 <sub>cold</sub>	bar	10.67	3.34	0.74	0.36	0.23

Table 11

Global warming potential for the three case studies.

	Case 1	Case 2	Case 3
$GWP_{leakage} [/\text{yr}], 5\%$	2009	1422	1707
$GWP_{CO2} [/\text{yr}]$	313,820	317,490	292,409
$GWP_{annual} [/\text{yr}]$	315,829	318,912	294,116
	Case 1	Case 2	Case 3
$GWP_{leakage} [/\text{yr}], 10\%$	4018	2844	3414
$GWP_{CO2} [/\text{yr}]$	313,820	317,490	292,409
$GWP_{annual} [/\text{yr}]$	317,838	320,334	295,823
	Case 1	Case 2	Case 3
$GWP_{leakage} [/\text{yr}], 15\%$	6027	4266	5121
$GWP_{CO2} [/\text{yr}]$	313,820	317,490	292,409
$GWP_{annual} [/\text{yr}]$	319,847	321,756	297,530

**Table 12**  
Estimation of Global Warming Potential for disposal.

	Volume [m <sup>3</sup> ]	Density [kg/m <sup>3</sup> ]	Inventory [kg]	Total inventory [kg]	Disposal [kg]	GWP <sub>MR</sub>	GWP <sub>disposal</sub>
Case 1	0.97	619.9	603.4	1436.7	431	8.5	3663.7
Case 2	0.66	936	616.7	1468.4	440.5	5	2202.6
Case 3 <sub>warm</sub>	0.79	1268.1	999.2	2379.1	713.7	1.7	1177.7
Case 3 <sub>cold</sub>	0.78	716.2	559.7	1332.7	399.8	8.5	3382.3

the GWP<sub>leakage</sub> is much smaller than GWP<sub>CO<sub>2</sub></sub>, so the annual GWP mainly depends on GWP<sub>CO<sub>2</sub></sub>. Although the GWP<sub>leakage</sub> in Case 2 is smaller than that in Case 1 due to the low GWP of HFO refrigerants, it cannot make the annual GWP in Case 2 lower than that of Case 1 because Case 2 has much higher GWP<sub>CO<sub>2</sub></sub> due to its higher energy consumption. On the other hand, Case 3 clearly shows the lowest annual GWP, because it consumes the smallest amount of energy, so GWP<sub>CO<sub>2</sub></sub> is the smallest. This means that the use of low GWP materials for refrigerants may not necessarily contribute to reducing the annual GWP, if the process efficiency is reduced by using low GWP materials. Instead, keeping low SEC is more effective to decrease the annual GWP even with high GWP type refrigerants.

Table 12 shows the volume of the heat exchanger, refrigerant density, inventory, and GWP<sub>disposal</sub>, which is generated when the refrigerant is disposed of after its lifespan. The total inventory of Case 1 and Case 2 are similar, but due to the difference in the value of GWP, Case 2 has a lower GWP<sub>disposal</sub> than that of Case 1. Case 3 uses two refrigeration cycles, and this makes the MR mass flowrate and GWP<sub>disposal</sub> larger than those of Cases 1 and 2 although it has a much lower GWP. Table 13 shows the total GWP of each case during 20 years using results from Tables 11 and 12 and Eq. (16). The GWP increases slightly with the leakage rate of refrigerants. However, it can be seen that the total GWP is still in the order of the lowest energy consumption regardless of the GWP leakage amount. This result shows that, when evaluating the impact of

**Table 13**  
Total Global Warming Potential variation with refrigerant leakage.

	Case 1	Case 2	Case 3
GWP <sub>total</sub> , leakage 5%	6,320,244	6,380,443	5,886,880
GWP <sub>total</sub> , leakage 10%	6,360,424	6,408,883	5,921,020
GWP <sub>total</sub> , leakage 15%	6,400,604	6,437,323	5,955,160

refrigerants on global warming, it is crucial to prioritize the energy loss caused by refrigerant replacement over the properties of the refrigerant itself.

#### 4.4. Summary of results

Fig. 9 shows the results of this study in graphical form. GWP<sub>total</sub> is estimated by assuming that leakage represents 5% of the mass flowrate of the refrigerant, and the overpressure is given at 10 m. When HFO refrigerants replace hydrocarbon in the SMR process, energy consumption of the re-liquefaction process is similar to the case of using HC-MR and the overpressure can greatly reduce due to lower combustion heat of HFO refrigerants. However, since the energy of the process was not reduced, GWP<sub>total</sub> did not decrease, although HFO refrigerants have less GWP than hydrocarbons. In the DMR process, energy consumption of the process decreases and HFO refrigerants can reduce overpressure and GWP<sub>total</sub>. However, there is a limit that this is due to the increased heat exchange efficiency using the DMR process rather than the characteristics of the HFO refrigerant. Also, there is no actual application case in using HFO refrigerant in the liquefaction process as studied in previous studies and present study. Appropriate experiments are needed to demonstrate the use of HFO refrigerants. When the DMR process is adopted to reduce the energy consumption and GWP of the process, it is necessary to evaluate the economic feasibility of the profit and loss according to the increasing CAPEX and decreasing OPEX.

## 5. Conclusion

In this study, we focused on assessing the feasibility of using HFO refrigerants as an eco-friendly and low-flammable alternative to propane and butane in BOG re-liquefaction processes. The SMR and DMR processes were optimized to minimize specific energy consumption

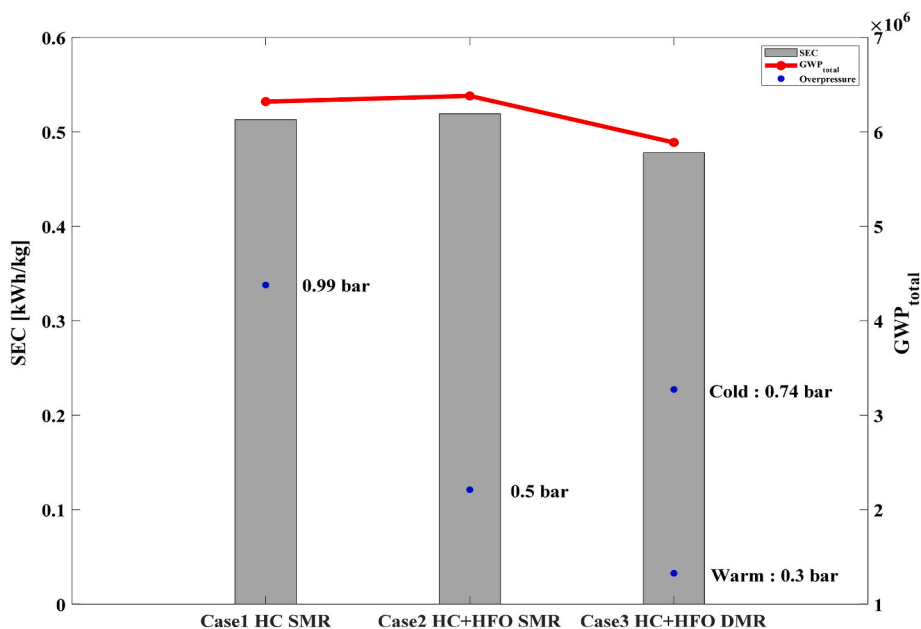


**Fig. 9.** Key performance indicators for the case studies.

(SEC) using particle swarm optimization (PSO). The TNT equivalency method was used to estimate the overpressure in the event of an explosion. The total global warming potential (GWP) during the lifespan of the BOG re-liquefaction process was estimated, considering refrigerant leakage, energy consumption, and disposal of refrigerants.

In conclusion, the utilization of HFO refrigerants in the BOG re-liquefaction process for LNG carriers presents both advantages and disadvantages. The BOG re-liquefaction process using HFO refrigerants has energy consumption comparable to that of the conventional hydrocarbon refrigerant-based process. The difference in energy consumption between Case 1 and Case 2 was only approximately 1%. The use of HFO refrigerant in the DMR process resulted in increased heat exchange efficiency due to the more efficient heat exchange between the two cooling loops, which led to a 7% reduction in energy consumption compared to the previous two cases. Additionally, it has the potential to reduce overpressure in the event of an explosion accident. The overpressure of the SMR process using HFO-based refrigerants (Case 2) can be reduced by 33.3%–49.5%, varying with the distance from the explosion center compared to Case 1. For Case 3, overpressure is decreased by 54.2–73.3% and 3.7–25.3% for warm and cold MR, respectively.

However, even when using environmentally-friendly HFO refrigerants, the overall reduction in GWP was not achieved due to the fact that CO<sub>2</sub> emissions resulting from energy consumption constitute the majority of the overall Global Warming Potential. After being applied to the DMR process, HFO refrigerants can reduce the total GWP. However, this reduction in GWP is limited by the fact that it stems more from the process efficiency improvement rather than the effect of HFO refrigerants. This indicates that for a truly environmentally-friendly re-liquefaction process design, the focus should be on the varying energy consumption associated with the use of different refrigerants, rather than on the own properties of the refrigerants.

## Nomenclature

### Abbreviations

ASHRAE = American Society of Heating, Refrigerating and Air-conditioning Engineers  
 BOG = Boil-off gas  
 BOR = Boil-off rate  
 DMR = Dual mixed refrigerant  
 GWP = Global warming potential  
 HC = Hydrocarbon  
 HFO = Hydrofluoroolefin  
 LNG = Liquefied natural gas  
 MR = Mixed refrigerant  
 NG = Natural gas  
 SMR = Single mixed refrigerant  
 SEC = Specific energy consumption [kWh/kg]

### Variables

$GWP_{leakage}$  = GWP generated by refrigerant leakage  
 $GWP_{CO_2}$  = GWP generated by power consumption for the re-liquefaction cycle  
 $GWP_{disposal}$  = GWP generated by refrigerant make-up.  
 $GWP_{total}$  = GWP generated during lifespan of ship.  
 $l$  = engine load [%]  
 LHV = lower heating value [kJ/kg]  
 $\dot{m}_{BOG}$  = mass flowrate of BOG generation [kg/hr]  
 $\dot{m}_{fuel}$  = mass flowrate of fuel [kg/hr]  
 $\dot{m}_{LNG}$  = mass flowrate of LNG production [kg/hr]  
 $\dot{m}_{MR}$  = mass flowrate of refrigerant [kg/hr]  
 $P_e$  = maximum engine power [kW]  
 SFOC = specific fuel oil consumption [kJ/kWh]  
 $\dot{W}_{comp}$  = refrigerant compression power [kW]

## CRedit authorship contribution statement

**Taejong Yu:** Conceptualization, Formal analysis, Methodology, Software, Investigation, Writing – original draft, Visualization. **Donghoi Kim:** Validation, Formal analysis, Investigation, Writing – review & editing. **Truls Gundersen:** Validation, Formal analysis, Investigation, Writing – review & editing, Supervision, Project administration. **Youngsub Lim:** Conceptualization, Formal analysis, Validation, Investigation, Writing – review & editing, Supervision, Project administration.

## Declaration of competing interest

The authors declare that they have no known competing financial interests or personal relationships that could have appeared to influence the work reported in this paper.

## Data availability

I specified the data and its resources in the manuscript.

## Acknowledgement

This research was supported by the MOTIE (Ministry of Trade, Industry, and Energy) in Korea, under the Fostering Global Talents for Innovative Growth Program (P0008747) supervised by the Korea Institute for Advancement of Technology (KIAT) and the Design/build a process for separation and recycling of unreacted CO<sub>2</sub> (0457–20210015) funded by the Ministry of Science and ICT through the National Research Foundation of Korea.

## References

- [1] IEA. World energy outlook 2019. 2019.
- [2] IGU. 2020 World LNG report. 2020.
- [3] IGU. 2020 World LNG report. 2023.
- [4] Lim Wonsub, Choi Kwangho, Moon Il. Current status and perspectives of liquefied natural gas (LNG) plant design. *Ind Eng Chem Res* 2013;52(9):3065–88.
- [5] Arias Fernández Ignacio, Romero Gómez Manuel, Romero Gómez Javier, BaalínAlnsua Álvaro. Review of propulsion systems on LNG carriers. *Renew Sustain Energy Rev* 2017;67:1395–411.
- [6] Hwang Chulmin, Lim Youngsub. Optimal process design of onboard BOG Re-liquefaction system for LNG carrier. *J Ocean EngTechnol* 2018;32(5):372–9.
- [7] Park Eunyoung, Choi Jungho. Greenhouse gas emission analysis by LNG fuel tank size through life cycle. *J Ocean EngTechnol* 2021;35(6):393–402.
- [8] Shin Younggy, Lee Yoon Pyo. Design of a boil-off natural gas reliquefaction control system for LNG carriers. *Appl Energy* 2009;86(1):37–44.
- [9] Son Hyunsoo, Kim Jin-Kuk. Energy-efficient process design and optimization of dual-expansion systems for BOG (Boil-off gas) Re-liquefaction process in LNG-fueled ship. *Energy* 2020;203:117823.
- [10] Lee Yoon-pyo, Shin You-hwan, Lee Sang-hoon, Kim Kwang-ho. Boil-off gas reliquefaction system for LNG carriers with BOG-BOG heat exchange. *J Soc Nav Archit Korea* 2009;46(4):444–51.
- [11] Romero-Gomez Manuel, Ferreiro García Ramón. On board LNG reliquefaction technology: a comparative study. *Pol Marit Res* 2013;21(1):77–88.
- [12] Romero Javier, Orosa José A, Oliveira Armando C. Research on the Brayton cycle design conditions for reliquefaction cooling of LNG boil off. *J Mar Sci Technol* 2012;17(4):532–41.
- [13] Yoo Junghyun, Lee Cheonkyu, Lee Jisung, Jeong Sangkwon. Exergy analysis of liquefied natural gas (LNG) boil-off gas (BOG) Re-liquefaction cycles for on-board application. In: *The twenty-fifth international ocean and polar engineering conference*. Hawaii, USA: Kona; June 2015.
- [14] Yin Liang, Ju Yonglin. Comparison and analysis of two processes for BOG reliquefaction in LNG carrier with normal-temperature compressor. *Int J Refrig* 2020;115:9–17.
- [15] Tan Hongbo, Shan Siyu, Yang Nie, Zhao Qingxuan. A new boil-off gas reliquefaction system for LNG carriers based on dual mixed refrigerant cycle. *Cryogenics* 2018;92:84–92.
- [16] Ting He, Lin Wensheng. Energy saving and production increase of mixed refrigerant natural gas liquefaction plants by taking advantage of natural cold sources in winter. *J Clean Prod* 2021;299:126884.
- [17] Yin QS, Li HY, Fan QH, Jia LX. Economic analysis of mixed-refrigerant cycle and nitrogen expander cycle in small scale natural gas liquifier. *AIP Conf Proc* 2008;985(1):1159–65.
- [18] ASHRAE. Designation and safety classification of refrigerant. In: *ANSI/ASHRAE standard 34-2010*. American Society of Heating, Refrigerating, and Air-Conditioning Engineers; 2010 (ASHRAE).
- [19] ASHRAE. Designation and safety classification of refrigerant. In: *ANSI/ASHRAE standard 34-2010*. American Society of Heating, Refrigerating, and Air-Conditioning Engineers; 2010 (ASHRAE).
- [20] Mota-Babiloni Adrian, Makhnatch Pavel. Predictions of European refrigerants place on the market following F-gas regulation restrictions. *Int J Refrig* 2021;127:101–10.
- [21] Wasim Akram M, Polychronopoulou Kyriaki, Polycarpoua Andreas A. Lubricity of environmentally friendly HFO-1234yf refrigerant. *Tribol Int* 2013;57:92–100.
- [22] Abdul Qyyum Muhammad, Lee Moonyong. Hydrofluoroolefin-based novel mixed refrigerant for energy efficient and ecological LNG production. *Energy* 2018;157:483–92.
- [23] Ali Wahid, Qadeer Kinza, Abdul Qyyum Muhammad, Hassan Alhazmi Waleed, Khan Mohd Shariq, Khan Mohd Shariq, Lee Moonyong. Thermo-economic assessment and uncertainty quantification of hydrofluoroolefin-based single mixed refrigerant process for natural gas liquefaction. Available at: SSRN. 2021. <https://doi.org/10.2139/ssrn.3899826>. <https://ssrn.com/abstract=3899826>.
- [24] Ahmad Naquash, Riaz Amjad, Lee Hyunhee, Abdul Qyyum Muhammad, Lee Sanggyu, Lam Su Shiung, Lee Moonyong. Hydrofluoroolefin-based mixed refrigerant for enhanced performance of hydrogen liquefaction process. *Int J Hydrogen Energy* 2022;47:41648–62.
- [25] Lee Hyunhee, Haider Junaid, Muhammad Abdul Qyyum, Choe Changgwon, Lim Hankwon. An innovative high energy efficiency-based process enhancement of hydrogen liquefaction: energy, exergy, and economic perspectives. *Fuel* 2022;320:123964.
- [26] Zhang Jinrui, Meerman Hans, Benders René, Faaij André. Comprehensive review of current natural gas liquefaction processes on technical and economic performance. *Appl Therm Eng* 2020;166:114736.
- [27] Vatani A, Mehrpooya M, Palizdar A. Energy and exergy analyses of five conventional liquefied natural gas processes. *Int J Energy Res* 2014;38(14):1843–63.
- [28] Venkatarathnam G. In: Timmerhaus KD, Rizzuto C, editors. *Cryogenic mixed refrigerant processes*. New York: Springer; 2008.
- [29] Lee Inkyu, Moon Il. Strategies for process and size selection of natural gas liquefaction processes: specific profit portfolio approach by economic based optimization. *Ind Eng Chem Res* 2018;57(17):5845–57.
- [30] Tian bao, Karimi Iftekhar A, Ju Yonglin. Review on the design and optimization of natural gas liquefaction processes for onshore and offshore applications. *Chem Eng Res Des* 2018;132:89–114.
- [31] Jonggeol Na, Lim Youngsub, Han Chonghun. A modified DIRECT algorithm for hidden constraints in an LNG process optimization. *Energy* 2017;126:488–500.
- [32] Kennedy J, Eberhart R. Particle swarm optimization. In: *Proceedings of ICNN'95 - international conference on neural networks*, vol. 4; 1995. p. 1942–8.
- [33] Eberhart R, Kennedy J. A New optimizer using particle swarm theory. *IEEE* 1995:39–43.
- [34] Khan Mohd Shariq, Lee Moonyong. Design optimization of single mixed refrigerant natural gas liquefaction process using the particle swarm paradigm with nonlinear constraints. *Energy* 2013;49(1):146–55.
- [35] Mokarizadeh Haghighi Shirazi M, Mowla D. Energy optimization for liquefaction process of natural gas in peak shaving plant. *Energy* 2010;35(7):2878–85.
- [36] Parker Sybil P. *Encyclopedia of science & technology*. sixth ed. New York: McGraw-Hill; 1987.
- [37] Center for Chemical Process Safety. *Guidelines for chemical process quantitative risk analysis*. second ed. 2000. New York.
- [38] Jan Babicz. *Wartsila encyclopedia of ship technology*. second ed. Wartsila; 2015.
- [39] Romero Gómez J, Romero Gómez M, Lopez Bernal J, Baalín Insua A. Analysis and efficiency enhancement of a boil-off gas reliquefaction system with cascade cycle on board LNG carriers. *Energy Convers Manag* 2015;94:261–74.
- [40] Winthertur Gas & Diesel Ltd. *Marine installation manual*. WINGD; 2020.
- [41] Wartsila. *Wartsila 34DF product guide*. Wartsila; 2020.
- [42] Aspen HYSYS Vvol. 10. 2020. Aspen Tech.
- [43] Matlab. 2019. *The Math Works, Inc.*
- [44] DNV. *Failure frequency guidance: process equipment leak frequency data for use in QRA*. 2012. Oslo, Norway.
- [45] Yoon Junghyun, Ha Jungchul, Ha Juchul. LNG vapour dispersion from atmospheric relief valve. Paris: *International Gas Union Research Conference*; 2008.
- [46] Park Sayyoon, Jeong Byongug, Lee Byung Suk, Oterkus Selda, Zhou Peilin. Potential risk of vapour cloud explosion in FLNG liquefaction modules. *Ocean Eng* 2018;149:423–37.
- [47] Frank P. Lees. *Loss prevention in the process industries : hazard identification assessment and control*. second ed. Oxford: Butterworth-Heinemann; 1996.
- [48] Trozzi C. *Emission estimate methodology for maritime navigation*. Rome: Techn Consulting; 2010.
- [49] Australian Energy Regulator. *National greenhouse accounts factors*. Australian Energy Regulator and Department of Environment of Australia; 2017.
- [50] EPA. *Direct fugitive emissions from refrigeration, air conditioning, fire suppression, and industrial gas*. 2014.
- [51] IRC. *Refrigerant inventory determination*. College of Engineering, University of Wisconsin-Madison; 2014.
- [52] Mehrpooya Mehdi, Sharifzadeh Mohammad Mehdi Moftakhari, Rosen Marc A. Optimum design and exergy analysis of a novel cryogenic air separation process with LNG (liquefied natural gas) cold energy utilization. *Energy* 2015;90:2047–69.